PROCEEDINGS OF SCIENCE

Most charming dibaryon near unitarity

Yan Lyu,[a,b,*] **Hui Tong,**[a,c] **Takuya Sugiura,**[c] **Sinya Aoki,**[d,b] **Takumi Doi,**[b,c] **Tetsuo Hatsuda,**[c] **Jie Meng**[a,e] **and Takaya Miyamoto**[b]

[a] *State Key Laboratory of Nuclear Physics and Technology, School of Physics, Peking University, Beijing 100871, China*

[b] *Quantum Hadron Physics Laboratory, RIKEN Nishina Center, Wako 351-0198, Japan*

[c] *Interdisciplinary Theoretical and Mathematical Sciences Program (iTHEMS), RIKEN, Wako 351-0198, Japan*

[d] *Center for Gravitational Physics, Yukawa Institute for Theoretical Physics, Kyoto University, Kyoto 606-8502, Japan*

[e] *Yukawa Institute for Theoretical Physics, Kyoto University, Kyoto 606-8502, Japan*

E-mail: helvetia@pku.edu.cn, tong16@pku.edu.cn, takuya.sugiura@riken.jp, saoki@yukawa.kyoto-u.ac.jp, doi@ribf.riken.jp, thatsuda@riken.jp, mengj@pku.edu.cn, miyamoto@ribf.riken.jp

We present a first study on a pair of triply charmed baryons, $\Omega_{ccc}\Omega_{ccc}$ in the ${}^1S_0$ channel, on the basis of the HAL QCD method. The measurements are perfomed on the $(2+1)$-flavor lattice QCD configurations with nearly physical light-quark masses and physical charm-quark mass. We show that the system with the Coulomb repulsion taking into account the charge form factor of Ω_{ccc} leads to the scattering length $a_0^{\rm C} \simeq -19$ fm and the effective range $r_{\rm eff}^{\rm C} \simeq 0.45$ fm, which indicates $\Omega_{ccc}\Omega_{ccc}$ is located in the unitary regime.

The 38th International Symposium on Lattice Field Theory, LATTICE2021 26th-30th July, 2021 Zoom/Gather@Massachusetts Institute of Technology

*Speaker

PoS(LATTICE2021)606

1. Introduction

Quest for dibaryon is one of the most challenging problems in nuclear and particle physics [1, 2]. Experimentally, the deuteron, composed of a proton and a neutron, is the only stable bound state. There are possible dibaryons composed of light quarks (u, d and s). In particular, a theoretical progress on the basis of lattice QCD (LQCD) simulations near the physical point has been made recently on the dibaryons with many strangeness, $p\Omega(uudsss)$ [3] and $\Omega\Omega(ssssss)$ [4].

Going beyond the light-quark sector, there are several studies on the charmed dibaryons from both phenomenological approach and LQCD approach [5–7]. In the charm-quark sector, although so far only the singly charmed baryon [8] and the doubly charmed baryon [9] have been observed, the triply charmed baryon Ω_{ccc} provides an ideal system to study the perturbative and nonperturbative aspects of QCD in the baryonic sector. Since it is predicted by Bjorken in 1980s [10], there are many studies on its mass and electromagnetic form factor (see [11] and references therein).

In this paper, we explore the charmed dibaryons, by focusing on its simplest possible form, $\Omega_{ccc}\Omega_{ccc}$ in the ${}^1S_0$ channel, from a first principle LQCD approach. In this specific channel, the maximum attraction is expected due to the Pauli exclusion between charm quarks at short distances does not operate when spin $s = 0$ and angular momentum $L = 0$. The HAL QCD method [12–14] is used to convert the spatial baryon-baryon correlation to the scattering parameters. As we will show latter, the $\Omega_{ccc}\Omega_{ccc}$ in the ${}^1S_0$ channel with the Coulomb repulsion is located near unitarity [15].

2. HAL QCD method

The equal-time Nambu-Bethe-Salpeter (NBS) amplitude $\psi(\boldsymbol{r})$, whose asymptotic behavior at large distances reproduces the scattering phase shift, plays an important role in the HAL QCD method [12–14], from which a non-local but energy-independent potential $U(\boldsymbol{r}, \boldsymbol{r}')$ can be defined. Since all the elastic scattering states are governed by the same potential $U(\boldsymbol{r}, \boldsymbol{r}')$, the time-dependent HAL QCD method [14] takes full advantage of all the NBS amplitudes below the inelastic threshold $\Delta E^* \sim \Lambda_{\rm QCD}$ by defining the R correlator as follows.

$$\begin{aligned} R(\boldsymbol{r}, t > 0) &= \sum_{\boldsymbol{x}} \langle 0|\hat{\Omega}_{ccc}(\boldsymbol{x}, t)\hat{\Omega}_{ccc}(\boldsymbol{r}+\boldsymbol{x}, t)\overline{\mathcal{J}}(0)|0\rangle \, / e^{-2m_{\Omega_{ccc}}t} \\ &= \sum_n A_n \psi_n(\boldsymbol{r}) e^{-(\Delta W_n)t} + O(e^{-(\Delta E^*)t}), \end{aligned} \tag{1}$$

with local interpolating operators $\hat{\Omega}_{ccc}$ and a wall-type source operator $\overline{\mathcal{J}}$. A_n is the overlapping factor defined by $\langle n|\overline{\mathcal{J}}(0)|0\rangle$, with $|n\rangle$ representing the QCD eigensates in a finite volume below the inelastic threshold, and $\Delta W_n = 2\sqrt{m^2_{\Omega_{ccc}} + \boldsymbol{k}_n^2} - 2m_{\Omega_{ccc}}$ with the baryon mass $m_{\Omega_{ccc}}$ and the relative momentum $\boldsymbol{k}_n$. The contributions from the inelastic states are exponentially suppressed when $t \gg (\Delta E^*)^{-1}$. As long as the condition for t is met, the R correlator can be shown to satisfy following integro-differential equation [14],

$$\left(\frac{1}{4m_{\Omega_{ccc}}}\frac{\partial^2}{\partial t^2} - \frac{\partial}{\partial t} + \frac{\nabla^2}{m_{\Omega_{ccc}}}\right) R(\boldsymbol{r}, t) = \int d\boldsymbol{r}' U(\boldsymbol{r}, \boldsymbol{r}') R(\boldsymbol{r}', t). \tag{2}$$

The effective central potential in the leading order approximation of the derivative expansion, $U(\boldsymbol{r},\boldsymbol{r}') = V(r)\delta(\boldsymbol{r}-\boldsymbol{r}') + \sum_{n=1} V_{2n}(\boldsymbol{r})\nabla^{2n}(\boldsymbol{r}-\boldsymbol{r}')$, is given by,

$$V(r) = \frac{1}{R(\boldsymbol{r},t)}\left(\frac{1}{4m_{\Omega_{ccc}}}\frac{\partial^2}{\partial t^2} - \frac{\partial}{\partial t} + \frac{\nabla^2}{m_{\Omega_{ccc}}}\right)R(\boldsymbol{r},t). \tag{3}$$

3. Lattice setup

$(2+1)$-flavor gauge configurations are generated on the 96^4 lattice with the Iwasaki gauge action at $\beta = 1.82$ and nonperturbatively $O(a)$-improved Wilson quark action with $c_{\rm sw} = 1.11$ and stout smearing [16]. The lattice spacing is $a \simeq 0.0846$ fm ($a^{-1} \simeq 2.333$ GeV), the pion mass and the kaon mass are $m_\pi \simeq 146$ MeV and $m_K \simeq 525$ MeV, respectively. We use the relativistic heavy quark (RHQ) action for the charm quark, which is designed to remove the leading order and the next-to-leading order cutoff errors [17]. Two sets of RHQ parameters [18] are used so as to interpolate the physical charm-quark mass and reproduce the dispersion relation for the spin-averaged $1S$ charmonium. The interpolated mass for Ω_{ccc} is $m_{\Omega_{ccc}} \simeq 4796$ MeV.

The measurements are performed by a combination of the Bridge++ code [19] and the unified contraction algorithm [20], where the former is used for the quark propagator and the latter is used for the contraction. The periodic (Derichlet) boundary condition is employed for spatial (temporal) direction. Four time measurements are performed by shifting the source position, where the Coulomb gauge fixing is imposed. Forward and backward propagation are averaged to reduce the statistical fluctuations. The total measurements is 112 configurations $\times$ 4 source positions $\times$ 2 (forward and backward).

4. Numerical results

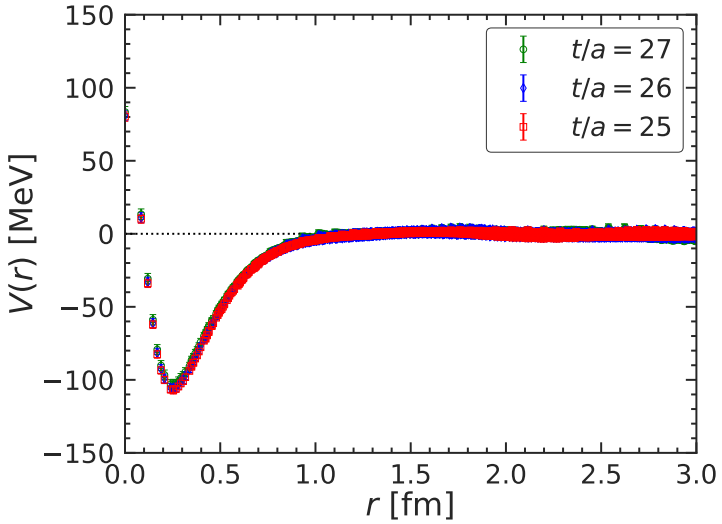

Figure 1: The $\Omega_{ccc}\Omega_{ccc}$ potential $V(r)$ in the ${}^1S_0$ channel at Euclidean time $t/a = 25$, 26, and 27.

In Fig. 1, we show the $\Omega_{ccc}\Omega_{ccc}$ potential $V(r)$ from the interpolation between two sets in the ${}^1S_0$ channel at Euclidean time $t/a = 25$, 26, and 27. The statistical errors for the potentials are

estimated by the jackknife method with a bin size of 14 configurations. The potentials for $t/a = 25$, 26, and 27 are nearly identical within statistical errors, which indicates systematic errors due to truncation of the derivative expansion and the inelastic states are small [14].

The potential $V(r)$ has qualitative features similar to NN potential [21] and $\Omega\Omega$ potential [4], i.e., a repulsive core surrounded by an attractive well. The magnitude of the repulsion for $\Omega_{ccc}\Omega_{ccc}$ is an order of magnitude smaller than that of $\Omega\Omega$, which is in line with the inverse ratio of the square of their constituent quark mass from the perspective of color-magnetic interaction [22]. In addition, the attraction, which may be attributed to the exchange of charmed mesons, is short-ranged.

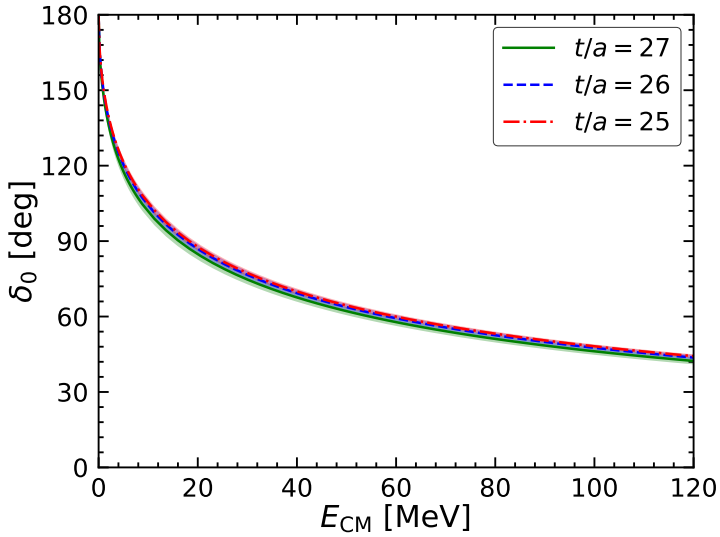

Figure 2: The scattering phase shifts δ_0 in the ${}^1S_0$ channel for $t/a = 25$, 26, and 27 as a function of the kinetic energy $E_{\rm CM} = 2\left(\sqrt{k^2 + m_{\Omega_{ccc}}^2} - m_{\Omega_{ccc}}\right)$ in the center of mass frame.

The $\Omega_{ccc}\Omega_{ccc}$ scattering phase shifts δ_0 in the ${}^1S_0$ channel calculated from the potential $V(r)$ at $t/a = 25$, 26, and 27 are shown in Fig. 2. The kinetic energy in the center of mass frame is defined as $E_{\rm CM} = 2\left(\sqrt{k^2 + m_{\Omega_{ccc}}^2} - m_{\Omega_{ccc}}\right)$. The phase shifts start from 180° indicates the existence of a bound state in the system without Coulomb repulsion.

Using the effective range expansion, $k \cot \delta_0 = -1/a_0 + 1/2 r_{\rm eff} k^2 + O(k^4)$ with the scattering length a_0 and the effective range $r_{\rm eff}$, we extract the low energy parameters as follows.

$$a_0 = 1.57(0.08)\left(^{+0.12}_{-0.04}\right)\ \text{fm}, \qquad r_{\rm eff} = 0.57(0.02)\left(^{+0.01}_{-0.00}\right)\ \text{fm}, \tag{4}$$

where the central values and the statistical errors in the first parentheses are extracted from δ_0 at $t/a = 26$, while the systematics errors in the second parentheses are estimated from the results at $t/a = 25$ and 27.

The binding energy B of the bound state is found to be $B \simeq 5.7$ MeV, and the corresponding root-mean-square distance is $\sqrt{\langle r^2 \rangle} \simeq 1.1$ fm. Since the binding energy and the size of the bound state from the strong interaction are not large, the Coulomb repulsion between two Ω_{ccc}^{++}s needs to be taken into account. Therefore, we consider the Coulomb repulsion $V^{\rm Coulomb}(r)$ by using the lattice results for the charge radius r_d of Ω_{ccc}^{++} in Ref. [11], $V^{\rm Coulomb}(r) = 4\alpha_e/rF(x)$ with $F(x) = 1 - e^{-x}(1 + 11x/16 + 3x^2/16 + x^3/48)$ and $x = 2\sqrt{6}r/r_d$. In order to see how the Coulomb

repulsion affects the system, we show the inverse of the scattering length $1/a_0^{\rm C}$ under the change of α_e from 0 to its physical value $\alpha_e^{\rm phys.} = 1/137.036$ in Fig. 3. At the physical point, i.e., $\alpha_e/\alpha_e^{\rm phys.} = 1$, the scattering parameters are,

$$a_0^{\rm C} = -19(7)\left(^{+7}_{-6}\right)\ \text{fm}, \qquad r_{\rm eff}^{\rm C} = 0.45(0.01)\left(^{+0.01}_{-0.00}\right)\ \text{fm}. \tag{5}$$

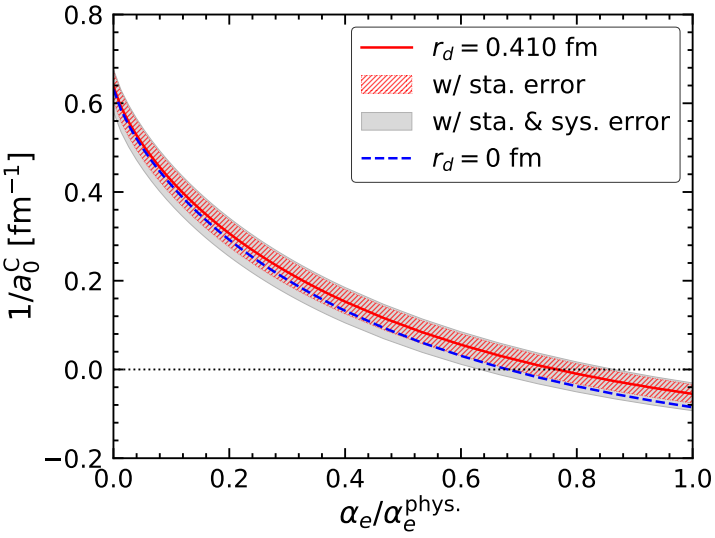

Figure 3: The inverse of the scattering length $1/a_0^{\rm C}$ as a function of $\alpha_e/\alpha_e^{\rm phys.}$. The red solid (blue dashed) line is the central values for $r_d = 0.410$ fm [11] ($r_d = 0$ fm). The inner (outer) band shows the statistical (statistical and systematic) errors.

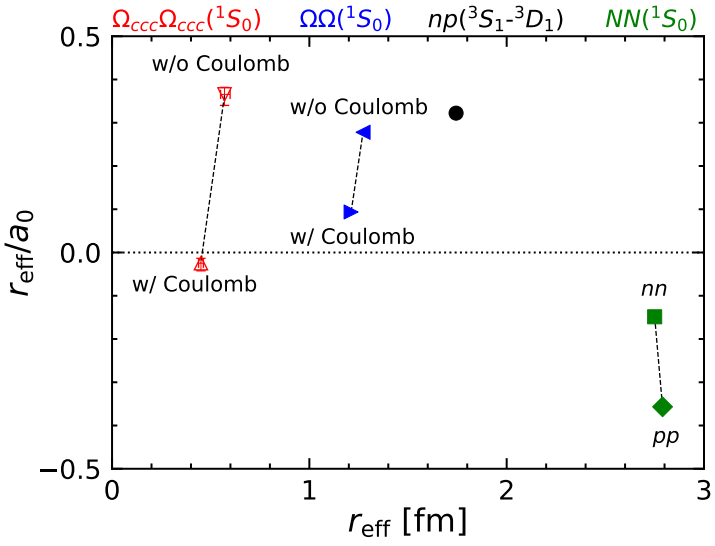

Figure 4: The dimensionless ratio $r_{\rm eff}/a_0$ as a function of $r_{\rm eff}$. The $\Omega_{ccc}\Omega_{ccc}$, $\Omega\Omega$, and NN in the $^1S_0$ channel with (without) Coulomb repulsion are shown by the red up(down)-pointing triangle, blue right(left)-pointing triangle, and green diamond (square) respectively. The black circle represents the $NN(^3S_1 - ^3D_1)$.

We plot the dimensionless ratio $r_{\rm eff}/a_0$ as a function of $r_{\rm eff}$ in Fig. 4. The $\Omega_{ccc}\Omega_{ccc}$, $\Omega\Omega$, and NN in the $^1S_0$ channel with (without) Coulomb repulsion are shown by the red up(down)-pointing

triangle, blue right(left)-pointing triangle, and green diamond (square) respectively. The black circle represents the $NN(^3S_1 - ^3D_1)$. Among all those dibaryons, $\Omega^{++}_{ccc}\Omega^{++}_{ccc}(^1S_0)$ is the closest to unitarity.

5. Summary

The $\Omega_{ccc}\Omega_{ccc}$ in the $^1S_0$ channel is studied for the first time on the basis of $(2+1)$-flavor lattice QCD simulations with nearly physical light-quark masses and physical charm-quark mass. The potential from the time-dependent HAL QCD method leads to a most charming ($C = 6$) dibaryon. By taking into account the Coulomb repulsion, the $\Omega^{++}_{ccc}\Omega^{++}_{ccc}(^1S_0)$ is found to be located in the unitary regime. It is an interesting future work to study $\Omega^{-}_{bbb}\Omega^{-}_{bbb}(^1S_0)$ to reveal the quark mass dependence of the scattering parameters.

Acknowledgements

We thank the members of HAL QCD Collaboration, the members of PACS Collaboration, Yusuke Namekawa, Tatsumi Aoyama, Haozhao Liang, Shuangquan Zhang and Pengwei Zhao for technical supports and stimulating discussions. We thank ILDG/JLDG [23] and the authors of cuLGT code [24]. The lattice QCD measurements have been performed on HOKUSAI supercomputers at RIKEN. This work was partially supported by HPCI System Research Project (hp120281, hp130023, hp140209, hp150223, hp150262, hp160211, hp170230, hp170170, hp180117, hp190103), the National Key R&D Program of China (Contracts Nos. 2017YFE0116700, 2018YFA0404400), the National Natural Science Foundation of China (Grant Nos. 11935003, 11975031, 11875075, 12070131001) , JSPS (Grant Nos. JP18H05236, JP16H03978, JP19K03879, JP18H05407), the MOST-RIKEN Joint Project "Ab initio investigation in nuclear physics", "Priority Issue on Post-K computer" (Elucidation of the Fundamental Laws and Evolution of the Universe), "Program for Promoting Researches on the Supercomputer Fugaku" (Simulation for basic science: from fundamental laws of particles to creation of nuclei), and Joint Institute for Computational Fundamental Science (JICFuS).

References

[1] H. Clement, Progress in Particle and Nuclear Physics **93**, 195 (2017).

[2] A. Gal, Acta Phys. Polon. B **47**, 471 (2016), arXiv:1511.06605 [nucl-th] .

[3] T. Iritani, S. Aoki, T. Doi, F. Etminan, S. Gongyo, T. Hatsuda, Y. Ikeda, T. Inoue, N. Ishii, T. Miyamoto, and K. Sasaki, Physics Letters B **792**, 284 (2019).

[4] S. Gongyo, K. Sasaki, S. Aoki, T. Doi, T. Hatsuda, Y. Ikeda, T. Inoue, T. Iritani, N. Ishii, T. Miyamoto, and H. Nemura (HAL QCD Collaboration), Phys. Rev. Lett. **120**, 212001 (2018).

[5] H. Huang, J. Ping, X. Zhu, and F. Wang, arXiv:2011.00513 [hep-ph] .

[6] J.-M. Richard, A. Valcarce, and J. Vijande, Phys. Rev. Lett. **124**, 212001 (2020).

[7] P. Junnarkar and N. Mathur, Phys. Rev. Lett. **123**, 162003 (2019).

[8] R. Aaij *et al.* (LHCb Collaboration), Phys. Rev. Lett. **118**, 182001 (2017).

[9] R. Aaij *et al.* (LHCb Collaboration), Phys. Rev. Lett. **119**, 112001 (2017).

[10] J. Bjorken, AIP Conf. Proc. **132**, 390 (1985).

[11] K. U. Can, G. Erkol, M. Oka, and T. T. Takahashi, Phys. Rev. D **92**, 114515 (2015).

[12] S. Aoki and T. Doi, Frontiers in Physics **8**, 307 (2020).

[13] N. Ishii, S. Aoki, and T. Hatsuda, Phys. Rev. Lett. **99**, 022001 (2007).

[14] N. Ishii, S. Aoki, T. Doi, T. Hatsuda, Y. Ikeda, T. Inoue, K. Murano, H. Nemura, and K. Sasaki (HAL QCD Collaboration), Physics Letters B **712**, 437 (2012).

[15] Y. Lyu, H. Tong, T. Sugiura, S. Aoki, T. Doi, T. Hatsuda, J. Meng, and T. Miyamoto, Phys. Rev. Lett. **127**, 072003 (2021).

[16] K.-I. Ishikawa, N. Ishizuka, Y. Kuramashi, Y. Nakamura, Y. Namekawa, Y. Taniguchi, N. Ukita, T. Yamazaki, and T. Yoshie (PACS), *Proc. Sci.* **LATTICE2015**, 075 (2016), arXiv:1511.09222 [hep-lat] .

[17] S. Aoki, Y. Kuramashi, and S.-i. Tominaga, Prog. Theor. Phys. **109**, 383 (2003), arXiv:hep-lat/0107009 .

[18] Y. Namekawa (PACS), *Proc. Sci.* **LATTICE2016**, 125 (2017).

[19] `http://bridge.kek.jp/Lattice-code/index_e.html`.

[20] T. Doi and M. G. Endres, Computer Physics Communications **184**, 117 (2013).

[21] T. Doi *et al.*, *Proc. Sci.* **LATTICE2016**, 110 (2017), arXiv:1702.01600 [hep-lat] .

[22] M. Oka, K. Shimizu, and K. Yazaki, Nuclear Physics A **464**, 700 (1987).

[23] `http://www.lqcd.org/ildg` and `http://www.jldg.org`.

[24] M. Schrock and H. Vogt, Computer Physics Communications **184**, 1907 (2013).